The International Journal of Cardiovascular Imaging **17:** 371–381, 2001.

A novel realistic three-layer phantom for intravascular ultrasound imaging

Jean Brunette[1], Rosaire Mongrain[1,2], Guy Cloutier[3], Michel Bertrand[4], Olivier F. Bertrand[5] & Jean-Claude Tardif[1]

[1]*Montreal Heart Institute;* [2]*McGill University;* [3]*University of Montreal Hospital;* [4]*École Polytechnique de Montréal;* [5]*Quebec Heart Institute, Montreal, Quebec, Canada*

Received 30 November 2000; accepted in revised form 2 July 2001

Key words: intravascular ultrasound, medical imaging, phantom, tissue characterization

Abstract

Intravascular ultrasound (IVUS) is an imaging modality that experienced a tremendous development over the last 20 years. Phantoms for IVUS are rare and poorly documented. The aim of this paper is to propose an original IVUS phantom that has geometries and specular textures closer to those of coronary arteries than conventional tube-like phantoms. The proposed phantom has a three-layer aspect, reproducing the intima, media and adventitia that compose the arterial wall. It is made of an agar-based compound, with water, glycerol and cellulose particles. Fourteen phantoms were quantified using IVUS. Six phantoms were evaluated by both photomacroscopy and IVUS. There was an excellent correlation between phantom dimensions evaluated by photomacroscopy and the nominal values (mold dimensions). The IVUS quantification of the phantom was closely correlated to the measurements obtained by photomacroscopy. These results demonstrate that a multilayer phantom, with known and reproducible dimensions and with realistic geometric and echographic properties has been developed.

Introduction

Intravascular ultrasound (IVUS) imaging is a high-resolution real-time tomographic modality that allows visualization of both arterial lumen and wall structures, improving on the limitations of angiography [1] that only provides a view-dependent two-dimensional projection of the lumen. IVUS allows a better understanding and assessment of coronary artery disease and particularly of plaque progression or regression, and response to various forms of therapy. It also offers a better guidance for balloon sizing, instrument selection and optimal stent deployment [2]. The value of IVUS, however, largely depends on the reliability of the measurements that it provides.

By comparing the dimensions of an object measured with a specific imaging modality, with the true dimensions, it is possible to determine the reliability of the imaging chain and its value for quantification. Phantoms are necessary to perform periodic verification of any imaging device calibration, as part of a quality control schedule. Ideally, each transducer should be calibrated prior to an IVUS study, much as pressure transducers are calibrated before each use [2]. Phantoms are important to compare imaging modalities, evaluate their limitations, and validate different algorithms such as automated segmentation of the different artery layers. An IVUS phantom can also be useful for a better understanding of image formation and material's response to ultrasonic interrogation. Phantoms can be used for the study of tissue characterization [3] and may also allow to reduce interobserver and interinstitutional variability in multicenter clinical studies or when

using more than one core laboratory in such trials [4].

Simple tubes [5] and catheters [6] have been reported as IVUS phantoms, but those have very little similarity with in vivo characteristics and echographic properties of arterial tissues. As shown in Figure 1, tubes can reproduce neither the texture nor the geometry of the different layers of the artery. Other structures have also been used including rubber O rings [7], casts from arteries [8, 9], wires [10], threads [11] and drilled holes in blocks [12]. A phantom adapted for IVUS should allow insonification from the lumen (internal flow area), feature dimensions reproducing in vivo morphology and show the different layers of the arterial wall structure (intima, media and adventitia). Although phantoms have been developed for Doppler and transcutaneous ultrasonography, there is scarce information about an endovascular phantom that could simulate the typical three-layer appearance of the vessels, with different stenosis severity, and typical clinical characteristics such as eccentricity. The aim of the present paper is to describe a new realistic coronary artery phantom adapted to IVUS imaging, having known and reproducible dimensions, showing geometric and echographic properties that are more realistic than presently available IVUS phantoms, and to evaluate its utility for dimension measurements.

Material and methods

Phantom geometry

Since a realistic phantom should reproduce the anatomy of human arteries, a mold had to be designed. This mold was machined in aluminum, because this metal is more durable than plastic, easy to machine, and also allows using heat-curing compounds. The mold was made of a male piece and a two-piece female, in order to extract more easily the phantom from the mold (Figure 2). The molding of the phantom was comparable to that of the plastic injection process by which a compound is poured in a female piece. The male is then forced in the female and the excess of material is evacuated. The remaining material takes the geometry of

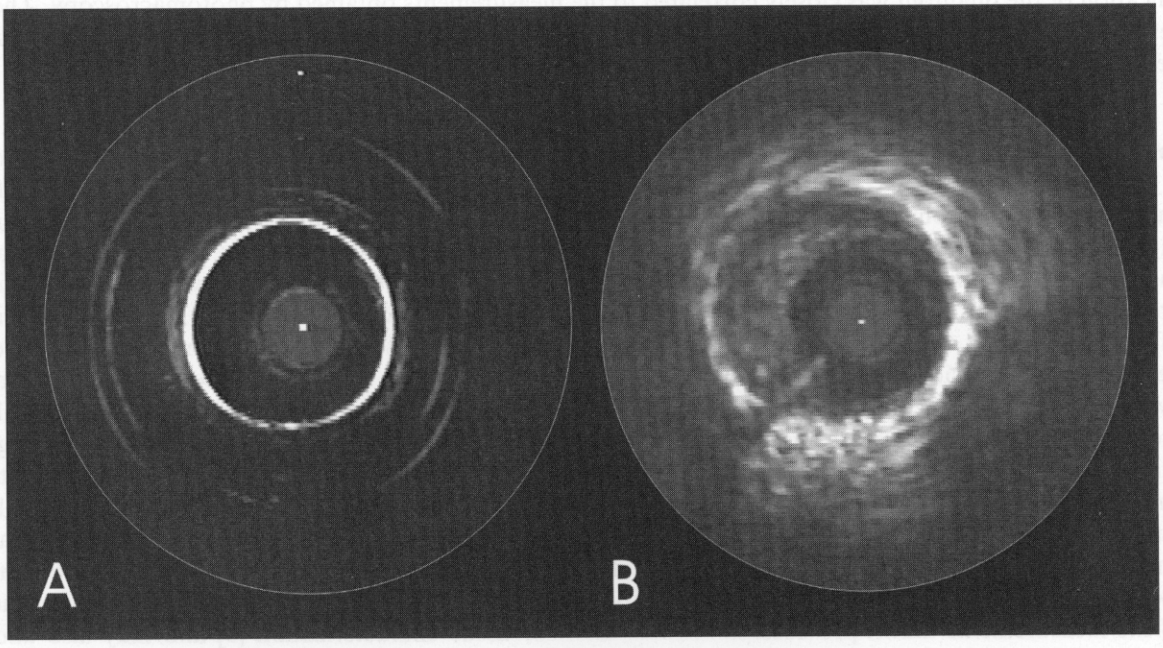

Figure 1. IVUS image of a silicone tube (A) as compared to the IVUS image of an in vivo coronary artery (B). Tubes and catheters are often used as phantoms, but their textures, geometries and echographic properties are different than those of real coronary arteries.

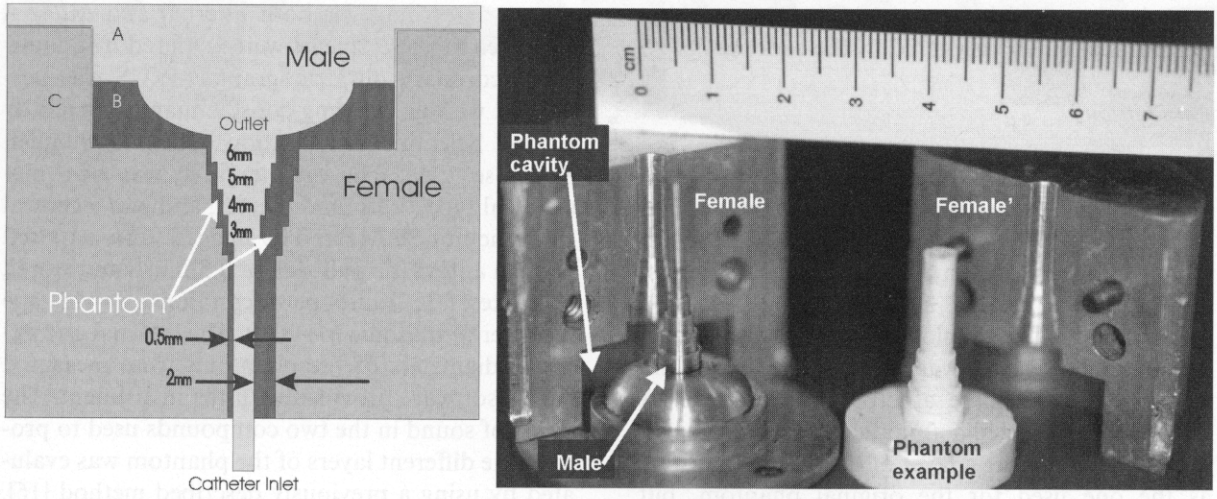

Figure 2. Schematic of the mold (left) in which the male piece (A), the female pieces (C), and the phantom (B) occupying the gap between the two parts are identified. The region of interest of the phantom is the center section in which we can observe internal diameters of 3, 4, 5, 6 mm and external diameters of 5.5, 6.5, 7.5 and 8.5 mm. Note the offset of the central axis of the male to that of the female, resulting in a wall thickness ranging from 0.5 mm on one side to 2 mm on the other side. The picture (right) illustrates the different pieces of the mold, and a sample of the original phantom in reference to a ruler (centimeters).

the cavity between the male and the female. The mold was designed to have four internal diameters (3, 4, 5, 6 mm) reproducing the range of lumen diameters, and four external diameters (5.5, 6.5, 7.5, 8.5 mm) for the range of total arterial diameters, as observed in human coronary and peripheral arteries. The axis of the male was offset to that of the female, therefore giving a non-uniform thickness to the wall, ranging from 500 μm to 2 mm. By having such offset, an asymmetric plaque was reproduced, as observed clinically in more than 74% of plaques [13, 14]. A tubular inlet allowed proper insertion of the catheter in the center of the phantom lumen and alignment parallel to the phantom symmetry axis. The concentricity of the catheter with respect to the axis of the phantom prevents some intensity artefacts and a nul angulation prevents geometric artefacts [15]. Indeed, the objective of the phantom is to evaluate the accuracy of the imaging chain alone and not the artefacts caused by the eccentricity and the angulation of the catheters, which have been studied in different investigations.

The four parts with internal diameters of 3, 4, 5 and 6 mm and the four parts having external diameters of 5.5, 6.5, 7.5 and 8.5 mm, were positioned in a way that the transition zones of the internal and external diameters were not located at the same site along the longitudinal axis. This allowed increasing the number of different combinations of internal and external diameters. The thick conic section on the upper part of the phantom was designed to increase mechanical structural strength.

Compound preparation

The compound prepared to create the phantom consisted of 5 ml of glycerol, 8 g of high strength agar gel (Sigma Chemical, St Louis, MO, A-6924), 1.5 g of cellulose particles (Sigma Chemical, St Louis, MO, 50 μm, S-5504) and 100 ml of water. This compound was used to simulate the intima and the adventitia layers. The media was created with the same compound but without scatterers (cellulose particles), in order to obtain an echolucent compound. Also, an additional 20 ml of water was necessary to decrease the viscosity of the compound in order to simulate the thin media. The media compound thus consisted of 5 ml of glycerol, 8 g of high strength agar gel and 120 ml of water. Both compounds had to be heated at 100 °C for 45 min. The heating process allows the compound to become more homogeneous, to release the

microbubbles and is important for the hardening process that will be triggered by the cooling.

Lamination

In order to reproduce the arterial layers observed in vivo, different layers were applied on the original phantom as it was when removed from the mold. This original phantom simulated the innermost arterial layer (intima) and was molded with a compound having cellulose particles as scatterers. This intima-like layer was relatively thick (500 μm to 2 mm), to simulate atherosclerotic plaque. A thin echolucent media (middle layer) was reproduced by laminating a layer of the same compound as the one used for the original phantom, but without cellulose scatterers. This lamination was produced by a brief dip of the phantom into the still warm compound solution. Once that thin echolucent layer was applied and set, a third layer with the same compound used for the original phantom was applied (with scatterers), again by a brief dip into the still warm compound. This last layer, simulating the adventitia, was easily differentiable from the middle one because of the presence of diffusion particles (cellulose). The resulting phantoms were evaluated by photomacroscopy and IVUS, in order to verify the accuracy and reproducibility of their dimensions. All measurements were performed on the internal and external borders of the original phantom, without the two outer layers since those are not molded but laminated and therefore less reproducible. The reproducibility of the media-like layer is dependent upon the viscosity of the still-warm compound which is initially in a liquid phase during the dipping.

Ultrasonography

A total of 14 phantoms immersed in water at 22 °C were quantified by IVUS. For every phantom, internal and external diameters of the different sections along the longitudinal axis of the original phantom were evaluated by four evenly spaced readings (approximately 45° apart). For each section, an average diameter was calculated from the four readings, for both the internal and external diameters. A total of 560 (14 phantoms × 4 sections × 5 readings for both internal and external diameters) measurements were acquired by quantitative coronary ultrasonography. IVUS was performed with an imaging console manufactured by Boston Scientific Corporation (Clearview model, San Jose, CA). The catheter used was of a mechanical type, 3.2 F in diameter, and had a central frequency of 30 MHz. The images were acquired with an automatic pullback of 0.5 mm/s and stored at a rate of 30 frames per second on a SVHS tape recorder (Panasonic MD830). The internal and external diameters of the phantoms were measured with a software provided with the instrument. The speed of sound in the two compounds used to produce the different layers of the phantom was evaluated by using a previously described method [16]. The measurement system consisted of a water reservoir, a 10 MHz ultrasonic transducer (quality factor = 7), a wideband ultrasonic pulser-receiver (Panametrics Inc., Waltham, MA, model 5900 PR) and a high-frequency analog-to-digital computer board (Gage Applied Sciences Inc., Montreal, Canada, model 8500). By measuring the thickness of the agar-based compound material with a micrometer ($\cong$1 mm) and the resulting change of the echoes transit time when the compound sample was placed between the probe and the reflector, it was possible to calculate the speed of sound into the compound, knowing the speed of sound in water:

$$\Delta t = 2\text{thickness}(1/c_{\text{compound}} - 1/c_{\text{water}})$$

The speed of sound in water was measured by displacing over a known distance the probe away from the reflector. The change in transit time in water for the known distance allowed to calculate the speed of sound. All measurements were performed at room temperature over eight different samples for each of the two types of compound. A total of 16 samples were obtained from eight batches of compounds produced on different days.

Photomacroscopy

The apparatus consisted of a numeric camera mounted on a dissection microscope. Photomacroscopy was processed on a total of six of the 14 insonified phantoms. Images were saved on compact disc (640 × 480, 8 bits). A total of 24 sections

were evaluated and four evenly spaced measurements were again performed for each internal and external diameter. Ultrasonography was performed prior to the photomacroscopy analysis because this last technique required a destructive process in which the section was exposed to the camera. Slices of the phantom were cut until the section of interest was visible. Great care was taken to ensure that the phantom geometry was not altered by the razor blade. The cutting was done by sliding the blade in order to minimize the pressure of the blade on the phantom. The photomacroscopy device was made by Leica (Leica Microsystems Heidelberg GmbH, model number MZ12). The quantification software was Nothon Eclipse (Empix Imaging, Inc, Mississauga, ON, Canada, version V.5).

Results

Figure 3 shows IVUS images of the phantom as it appears after the molding (A), when immersed in blood mimic (B), and after lamination (C). All three layers are clearly differentiable. The media is thinner than the other layers, and echolucent as compared to the adventitia which is often difficult to distinguish from the surrounding tissues. The plaque is asymmetric, because of the offset between the male and female axes of the mold. Figure 4 shows images of the original phantom, acquired by photomacroscopy. The lumen is circular and the different parts of external diameters can easily be distinguished. It is also possible to observe the internal diameters by transparency of the material. The changes of the internal diameters are located in between the changes of the external diameters along the longitudinal axis. IVUS images of the multilayer phantom showed textures that are much closer to those observed in vivo as compared to tubes or currently developed phantoms made of machined plastic or uniform material. Figure 5 depicts some IVUS images of in vivo human coronary arteries as compared to the phantom. Figure 6 presents linear regression of the dimensions of the phantom evaluated by photomacroscopy as compared to the nominal values of the mold. Figure 7 represents linear regressions of the dimensions evaluated by IVUS as compared to those obtained by photomacroscopy.

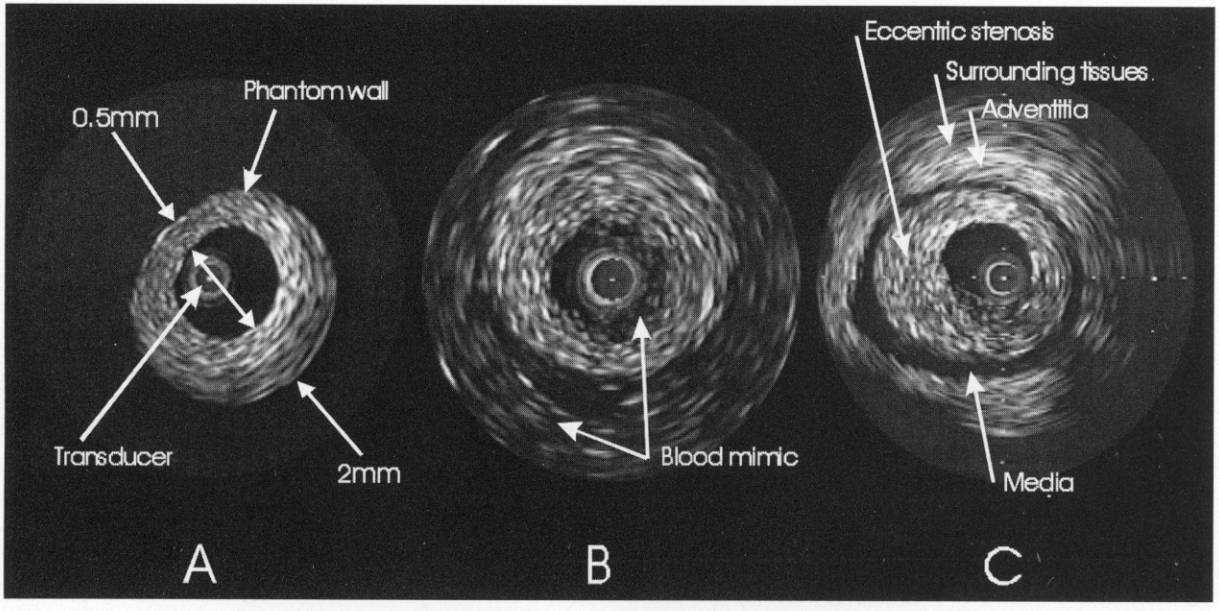

Figure 3. IVUS image of the proposed phantom as molded (A), immersed in blood mimic (B), and with the three-layer aspect after lamination (C).

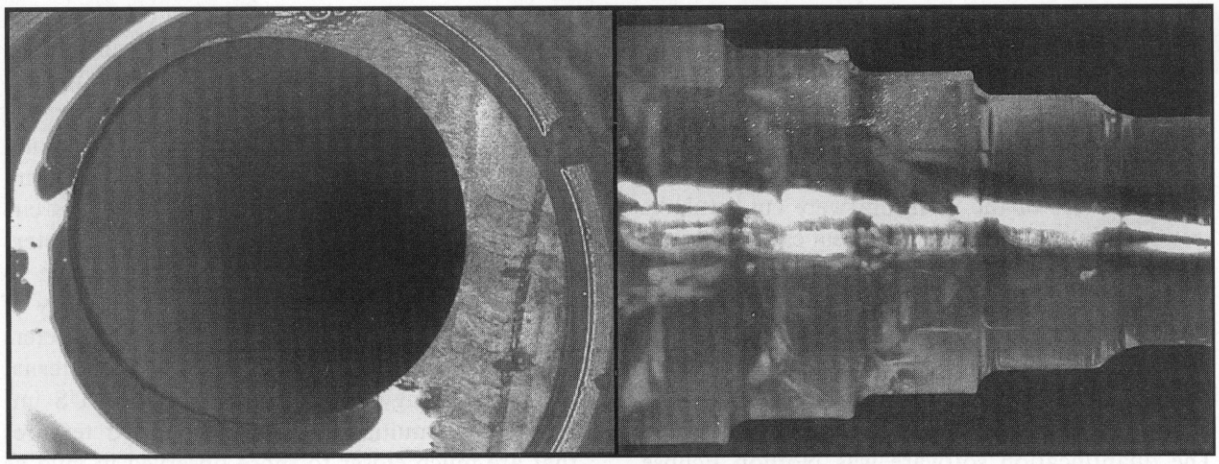

Figure 4. Image of the original phantom (before lamination), acquired by photomacroscopy. On the left is an image of a transversal cut of the phantom, showing the uniform circularity of the internal diameter. On the right panel, an image of the exterior of the phantom, as seen per photomacroscopy, is provided. The different external diameters of the original phantom are depicted.

The linear regression analysis performed to compare the measurements obtained by photomacroscopy with the nominal dimensions demonstrated that these two sets of data were highly related. The slopes were 0.98 and 0.99 for the internal and external diameters respectively. The average differences between the two sets of data were −0.6% and −0.1% for the internal and external diameters respectively, meaning that the phantom was slightly smaller than the nominal dimensions of the mold.

The IVUS measurements of the phantom were compared to those obtained by photomacroscopy. The linear regression analysis demonstrated a high relation between the two sets of data. The slopes obtained were 1.04 and 1.05 for the internal and external diameters respectively.

Figure 8(A) (top) represents the differences between the photomacroscopy and the nominal values plotted against the nominal values, in a Bland and Altman fasion [17]. The data is summarized into a mean difference and a standard deviation for each nominal diameter. Figure 8(B) (bottom) represents the differences between the ultrasonography and the photomacroscopy values plotted against the nominal values. Again, the data is summarized into a mean difference and a standard deviation for each nominal diameter.

Discussion

Phantom material

Many materials have previously been used for the elaboration of phantoms adapted to ultrasonography. Plexiglas [18], paraffin [19], silicone [20], polyvinyl chloride [21] and rubber [22] have been frequently chosen but cellophane [15], polyethylene [6], polyester [23] and plastic foam [24] have also been used. However, most of these materials have been used when only the internal interface (fluid–phantom) was of interest, and therefore attenuation and impedance were not of critical concerns. Since the objective of the proposed phantom was to allow the creation of an image of the different layers of the phantom wall, the impedance became important. For this reason, most of the above mentioned materials were inadequate. Silicone, paraffin, Plexiglas and rubber indeed have acoustical impedances much larger than those of water and biological soft tissues [25]. In contrast, an agar-based compound has previously been used for the creation of echography phantoms [26–29] and was described as having echographic properties that can be close to those of biological tissues. Ryan and Foster did not use any glycerol in their phantom. As scatterers, they utilized silica powder having an

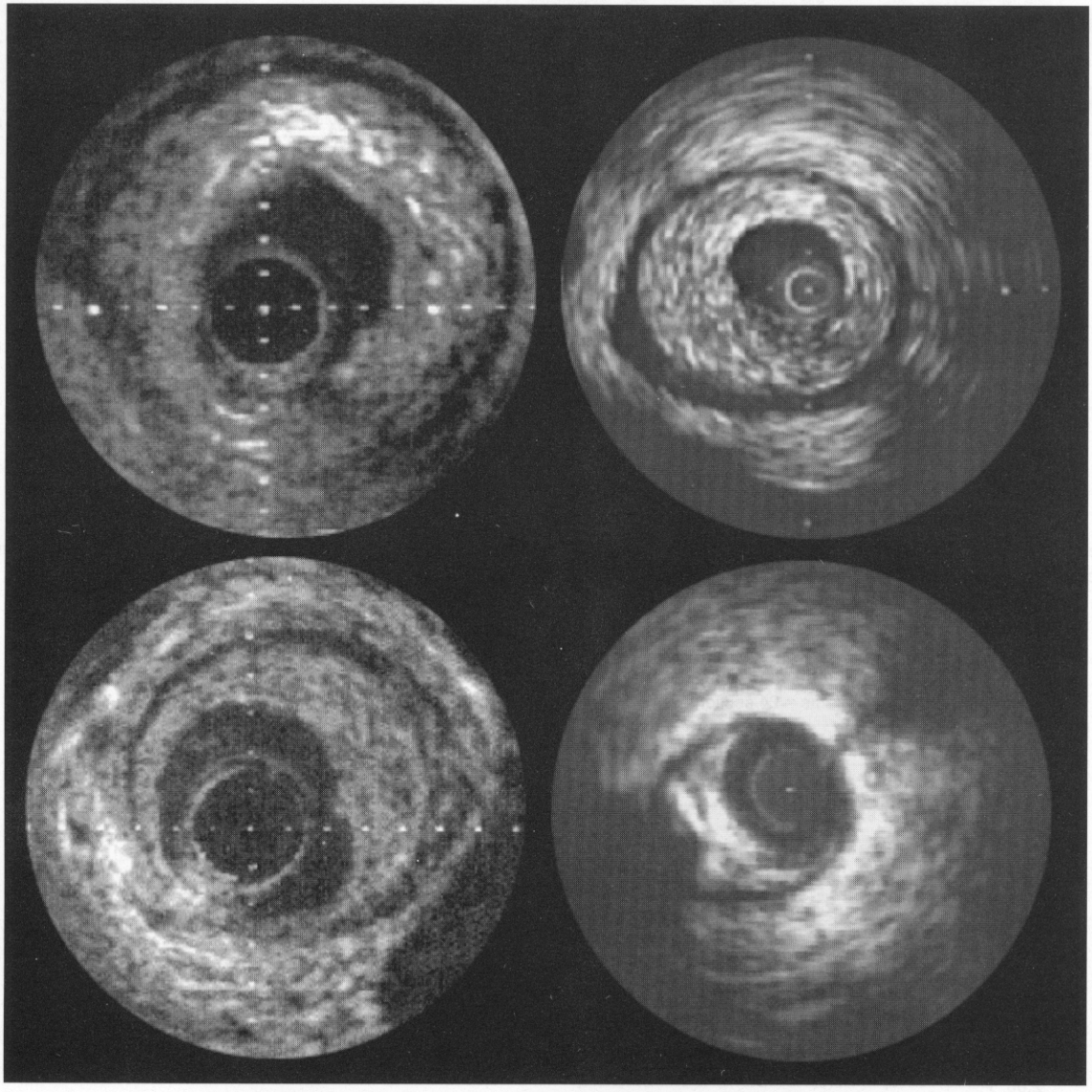

Figure 5. IVUS images of in vivo coronary arteries as compared to an IVUS image of the phantom (top right image).

average size between 1 and 5 μm in order to obey the Rayleigh statistics (particles diameter $<1/10$ of the wavelength). Images were obtained with a 42 MHz probe in their study. Rickey et al. used glycerol in order to control the speed of sound in their study. Their average scatterers size was 50 μm and their probe had a central frequency of 6 MHz. The compound preparation used for our phantom consisted in the one developed by Rickey et al. but adapted to IVUS. This adaptation was required to create a more resistant compound that would allow a 500 μm wall phantom to handle passage of the IVUS catheter. In our study, a 50 μm diameter cellulose particle powder was utilized to simulate the dimensions of the migrated smooth muscle cells and the foam cells mainly located in the intima. The sound velocity and the attenuation can be modified by addition of glycerol and scatterers respectively,

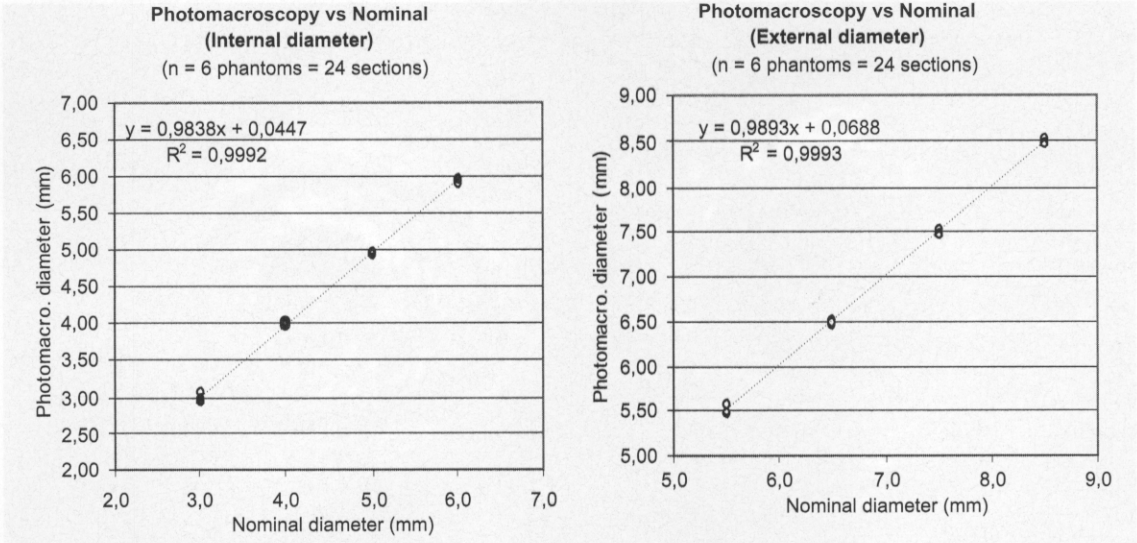

Figure 6. Linear regression of the internal diameters (left) and external diameters (right) of the phantom evaluated by photomacroscopy as compared to the nominal diameters of the mold.

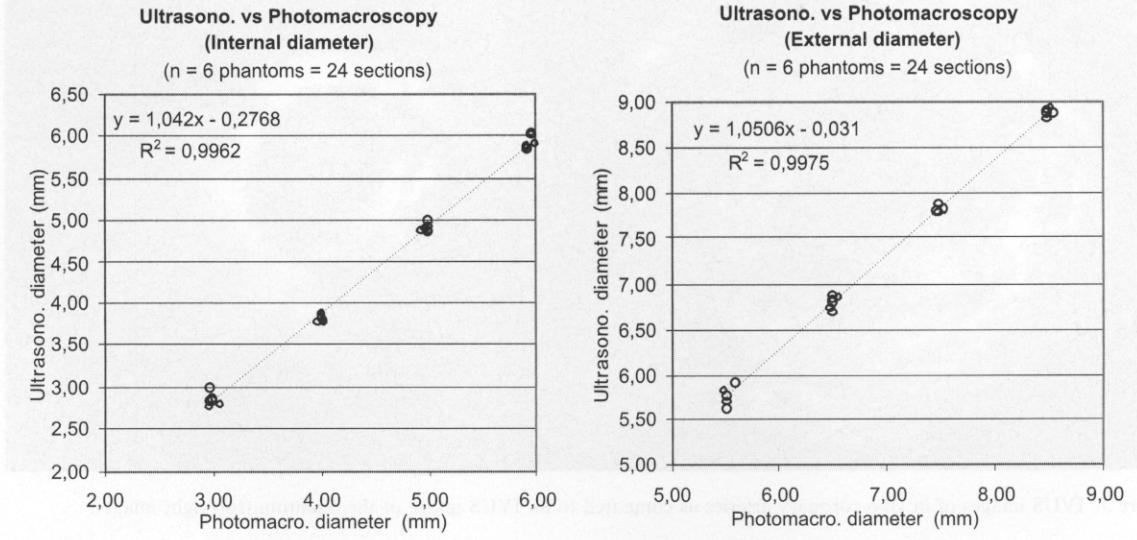

Figure 7. Linear regression of the internal diameters (left) and external diameters (right) of the phantom evaluated by ultrasonography as compared to those obtained by photomacroscopy.

therefore allowing to obtain the desired specifications.

Photomacroscopy vs. nominal values

One could expect that an object molded in a gap located between a male and a female piece would lead to an undersizing of the external dimensions and an oversizing of the internal dimensions, because of the molding process itself. In our study, the internal and external dimensions of the phantom were both slightly smaller than the mold, suggesting that the phantom may have shrunk. This small shrinkage might have been caused by

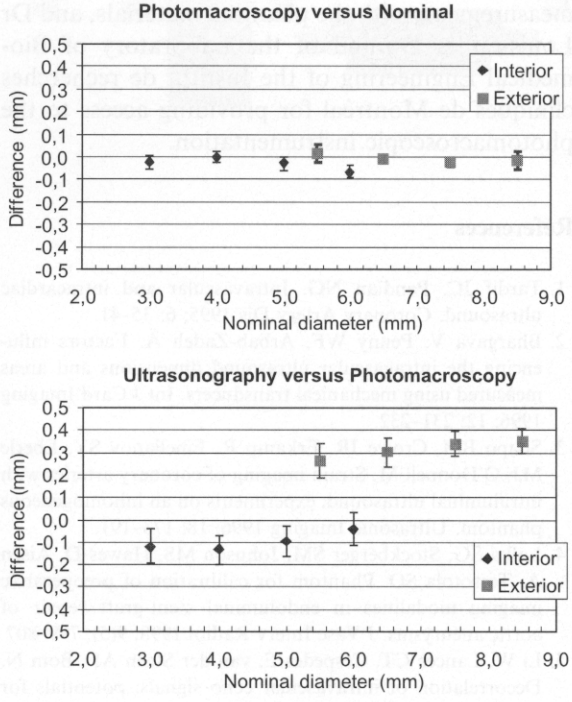

Figure 8. (A) (top): Differences between photomacroscopy and nominal values plotted against the nominal values. (B) (bottom): Differences between ultrasonography and photomacroscopy plotted against the nominal values.

the light beam generated by the lighting system of the microscope that warms and dehydrates the phantom material. This phenomenon might be responsible for the slight undersizing of the phantom (mean of 0.6% and 0.1% for the inside and the outside diameters respectively). In absolute values, these differences between photomacroscopy and nominal values were smaller than 0.1 mm over the entire range of diameters.

Ultrasonography vs. photomacroscopy

The average differences between both techniques revealed an underestimation of the internal diameters (−2.4%) and an overestimation of the external diameters (4.6%) by IVUS. This phenomenon may be explained by an increase of the phantom thickness due to water absorption. Indeed, the immersion of the phantom in water may cause a slight expansion of the phantom material, leading to an increase of the outside dimensions and a decrease of the inside dimensions. In addition, an overestimation of the transit times and distances occurred because the IVUS measurements were made in water instead of blood. A correction factor of 0.953 (−4.7%) was reported to counteract this phenomenon [30]. However, this correction factor should be considered for the distance covered in water, therefore in the lumen only. No correction factor has been applied on the data acquired in the present study because the sound travelled in both water and phantom in variable proportion for each section and for each angle. The speed of sound in the phantom (original phantom compound) was measured ($n = 8$) and was equal to 1534 ± 6 m/s (1528 ± 5 m/s for the echolucent compound, $n = 8$). The effect of temperature (22 °C vs. 37 °C) has been described as relatively negligible over a 15 °C difference as compared to the effect of the speed of sound in water vs. blood [30]. The speed of sound in blood at 37 °C has been reported to be 1540 m/s [18], 1560 m/s [25] and 1570 m/s [30], depending on different factors such as the haematocrit [18].

Limitations

In the current study, the validation was performed with the original phantom. Its reproducibility and accuracy were high because of the molding process. Although the compounds of the other layers were also very reproducible, their thicknesses were less obvious to reproduce from one phantom to another, because of the manual input to the laminating process and this may be considered a limitation. It is possible to overcome this limitation by molding the subsequent layers over the original phantom. The original phantom, once molded, could remain on the male piece of the mold in order to preserve its dimensions, whereas the female piece could be replaced by a larger one, machined to the desired external dimensions of the media-like layer. Similarly, the third and last layer could be molded over the previous ones. Nevertheless, the dimensions of the original phantom (internal and external) and its echographic properties provide a robust material to perform calibration.

Although this phantom was not designed to accommodate flow, an inlet and an outlet could be incorporated to support perfusion under pressure. The phantom could be reinforced by coating its exterior with a stronger layer, and its elasticity could be modified as desired. By creating compounds with different mechanical properties the phantom could be utilized to validate elastography-based tissue characterization algorithms. Further studies are planned to modify certain regions in the phantom by locally incorporating compounds having different echographic properties within the same layer in order to simulate calcified nests or lipid pools for instance. This would be of great interest to validate tissue characterization techniques.

Conclusion

A phantom for IVUS imaging was molded with a compound made of agar, glycerol, cellulose particles as scatterers, and water. This phantom was laminated with compounds having different echographic properties to reproduce the characteristics of the different layers of coronary and peripheral arteries. The offset of the male axis of the phantom to that of the female reproduced an asymmetric stenosis. This phantom simulating coronary arteries as observed in clinical practice demonstrated that it is possible to obtain a robust and reproducible IVUS multilayer phantom featuring much more realistic geometry and ultrasonic properties than currently developed phantoms. Studies by quantitative ultrasonography and photomacroscopy have proven the original phantom to be highly reproducible and precise. The phantom could be used to calibrate IVUS devices and to validate automated segmentation algorithm or tissue characterization techniques.

Acknowledgments

The authors would like to acknowledge Mr David Savéry of the Laboratory of Biorheology and Medical Ultrasonics of the University of Montreal Hospital for performing the acoustic velocity measurements with the phantom materials, and Dr Louis-Gilles Durand of the Laboratory of Biomedical Engineering of the Institut de recherches cliniques de Montréal for providing access to the photomacroscopic instrumentation.

References

1. Tardif JC, Pandian NG. Intravascular and intracardiac ultrasound. Coronary Artery Dis 1995; 6: 35–41.
2. Bhargava V, Penny WF, Arbab-Zadeh A. Factors influencing the intravascular ultrasound dimensions and areas measured using mechanical transducers. Int J Card Imaging 1996; 12: 231–232.
3. Shapo BM, Crowe JR, Erkamp R, Emelianov SY, Eberle MJ, O'Donnell M. Strain imaging of coronary arteries with intraluminal ultrasound: experiments on an inhomogeneous phantom. Ultrasonic Imaging 1996; 18: 173–191.
4. Lalka SG, Stockberger SM, Johnson MS, Hawes D, Aisen A, Trerotola SO. Phantom for calibration of preoperative imaging modalities in endoluminal stent-graft repair of aortic aneurysms. J Vasc Interv Radiol 1998; 9(5): 799–807.
5. Li W, Lancée CT, Cespedes E, van der Steen AF, Bom N. Decorrelation of intravascular echo signals: potentials for blood velocity estimation. J Acoust Soc Am 1998; 102(6): 3785–3794.
6. Evans JL, Ng KH, Wiet SG, et al. Accurate three-dimensional reconstruction of intravascular ultrasound data: spatially correct three-dimensional reconstructions. Circulation 1996; 93(3): 567–576.
7. Kimura BJ, Bhargava V, Palinski W, Russo RJ, DeMaria AN. Distortion of intravascular ultrasound images because of nonuniform angular velocity of mechanical-type transducers. Am Heart J 1996; 132: 328–336.
8. Ng KH, Evans JL, Vonesh MJ, et al. Arterial imaging with a new forward-viewing intravascular ultrasound catheter, II: three-dimensional reconstruction and display of data. Circulation 1994; 89(2): 718–723.
9. Hoskin PR, McDicken N. Techniques for the assessment of the imaging characteristics of intravascular ultrasound scanners. Brit J Radiol 1994; 67: 695–700.
10. Engeler CE, Ritenour ER, Amplatz K. Axial and lateral resolution of rotational intravascular ultrasound: in vitro observations and diagnostic implications. Cardiovasc Intervent Radiol 1995; 18: 239–242.
11. Kearney P, Ramo P, Spencer T, et al. A study of the quantitative and qualitative impact of catheter shaft angulation in a mechanical intravascular ultrasound system. Ultrasound Med Biol 1997; 23(1): 87–93.
12. Evans JL, Ng KH, Vonesh MJ, et al. Arterial imaging with a new forward-viewing intravascular ultrasound catheter, I (initial studies). Circulation 1994; 89(2): 712–717.
13. Mintz GS, Popma J, Pichard AD, et al. Limitations of angiography in the assessment of plaque distribution in coronary artery disease. Circulation 1996; 93: 924–931.

14. Brown BG, Bolson EL, Dodge HT. Dynamic mechanisms in human coronary restenosis. Circulation 1984; 70(6): 917–922.
15. Finet G, Tabib A, Maurincomme E, et al. Artefacts and intravascular ultrasonography. Analysis and implications for a better reliability in the interpretation of images and measurements. Arch Mal Coeur Vaiss 1994; 87(2): 271–280.
16. Selfridge AR. Approximate material properties in isotropic materials. IEEE Trans on Sonics and Ultrasonics 1985; 32 (Suppl 3): 381–394.
17. Bland JM, Altman DG. Statistical methods for assessing agreement between two methods of clinical measurement. Lancet 1986; 1(8476): 307–310.
18. Stahr P, Rupprecht HJ, Voigtlanger T, et al. Importance of calibration for diameter and area determination by intravascular ultrasound. Int J Card Imaging 1996; 12: 221–229.
19. von Birgelen C, Di Mario C, Li W, et al. Morphometric analysis in three-dimensional intracoronary ultrasound: an in vitro and in vivo study performed with a novel system for the contour detection of lumen and plaque. Am Heart J 1996; 132(3): 516–524.
20. Chae JS, Brisken AF, Maurer G, Siegel RJ. Geometric accuracy of intravascular ultrasound imaging. J Am Soc Echocardiogr 1992; 5(6): 577–587.
21. Geselschap JH, Heilbron MJ, Hussains FM, et al. The effect of angulation on intravascular ultrasound imaging observed in vascular phantoms. J Endovasc Surg 1998; 5: 126–133.
22. Deane CR, Markus HS. Color velocity flow measurement: in vitro validation and application to human carotid arteries. Ultrasound Med Biol 1997; 23(3): 447–452.
23. Frayne R, Gowman LM, Rickey DW, et al. A geometrically accurate vascular phantom for comparative studies of X-rays, ultrasound, and magnetic resonance vascular imaging: construction and geometrical verification. Medical Physics 1993; 20(2): 415–425.
24. Barry CD, Allott CP, John NW, et al. Three-dimensional freehand ultrasound: image reconstruction and volume analysis. Ultrasound Med Biol 1997; 23(8): 1209–1224.
25. Wells P. Biomedical Ultrasonics. Academic Press: New York, 1997.
26. Rickey DW, Picot PA, Christopher DA, Fenster A. A wall-less vessel phantom for Doppler ultrasound studies. Ultrasound Med Biol 1998; 21(9): 1163–1176.
27. Ryan LK, Foster FS. Tissue equivalent vessel phantom for intravascular ultrasound. Ultrasound Med Biol 1997; 23(2): 261–273.
28. Guo Z, Fenster A. Three-dimensional power doppler imaging: a phantom study to quantify vessel stenosis. Ultrasound Med Biol 1996; 22(8): 1059–1069.
29. Guo Z, Durand LG, Allard L, Cloutier G, Fenster A. In vitro evaluation of multiple arterial stenoses using three-dimensional power Doppler angiography. J Vasc Surg 1998; 27: 681–688.
30. von Birgelen C. Three-dimensional intravascular ultrasound assessment of coronary lumen and atherosclerotic plaque dimensions. Am Heart J 1996; 32: 516–527.

Address for correspondence: Jean-Claude Tardif, MD, Intravascular Ultrasound Laboratory, Montreal Heart Institute, 5000 rue Bélanger, Montreal, Qc, Canada H1T 1C8
Phone: +1-514-376-3330, ext. 3564; Fax: +1-514-593-2500;
E-mail: tardifjc@icm.umontreal.ca